



# Efficiency of photoprotection in microphytobenthos: role of vertical migration and the xanthophyll cycle against photoinhibition

Joao Serôdio, Joao Ezequiel, Alexandre Barnett, Jean-Luc Mouget, Vona Méléder, Martin Laviale, Johann Lavaud

## ► To cite this version:

Joao Serôdio, Joao Ezequiel, Alexandre Barnett, Jean-Luc Mouget, Vona Méléder, et al.. Efficiency of photoprotection in microphytobenthos: role of vertical migration and the xanthophyll cycle against photoinhibition. *Aquatic Microbial Ecology*, 2012, 67, pp.161-175. 10.3354/ame01591 . hal-01096446v2

**HAL Id: hal-01096446**

**<https://hal.science/hal-01096446v2>**

Submitted on 19 Dec 2014

**HAL** is a multi-disciplinary open access archive for the deposit and dissemination of scientific research documents, whether they are published or not. The documents may come from teaching and research institutions in France or abroad, or from public or private research centers.

L'archive ouverte pluridisciplinaire **HAL**, est destinée au dépôt et à la diffusion de documents scientifiques de niveau recherche, publiés ou non, émanant des établissements d'enseignement et de recherche français ou étrangers, des laboratoires publics ou privés.



Efficiency of photoprotection in microphytobenthos: the role of vertical migration and the xanthophyll cycle against photoinhibition

João Serôdio<sup>1,2\*</sup>, João Ezequiel<sup>1</sup>, Alexandre Barnett<sup>2</sup>, Jean-Luc Mouget<sup>3</sup>, Vona Méléder<sup>2,4</sup>, Martin Laviale<sup>1,4</sup>, Johann Lavaud<sup>2</sup>

<sup>1</sup> Departamento de Biologia and CESAM – Centro de Estudos do Ambiente e do Mar, Universidade de Aveiro, Campus de Santiago, 3810-193 Aveiro, Portugal

<sup>2</sup> UMR 7266 ‘LIENSs’, CNRS-University of La Rochelle, Institute for Coastal and Environmental Research (ILE), 2 rue Olympe de Gouges, 17 000 La Rochelle, France

<sup>3</sup> Mer Molécules Santé – MMS EA 2160, Université du Maine. Av. O. Messiaen, 72085 Le Mans Cedex 9, France

<sup>4</sup> Mer Molécules Santé – MMS EA 2160, Université de Nantes. BP 92 208, 44322, Nantes Cedex 3, France

\* Corresponding author: jserodio@ua.pt



## Abstract

The capacity of estuarine microphytobenthos to withstand the variable and extreme conditions of the intertidal environment, prone to cause photoinhibition of the photosynthetic apparatus, has been attributed to particularly efficient photoprotection mechanisms. However, little is known regarding its actual photoprotection capacity or the mechanisms responsible for the protecting against photoinhibition. This study addressed these questions by (i) quantifying the photoprotection capacity and the extent of photoinhibition under high light exposure, (ii) estimating the contribution of vertical migration and the xanthophyll cycle to overall photoprotection and (iii) evaluating the effects of photoacclimation state. A new experimental protocol was developed, combining (i) chlorophyll fluorescence imaging, for the simultaneous measurement of replicates and experimental treatments, (ii) specific inhibitors for vertical migration and for the xanthophyll cycle, to quantify the relative contribution of each process, and (iii) recovery kinetics analysis of photosynthetic activity during light stress-recovery experiments, to distinguish reversible downregulation from photoinhibition. The results showed a high photoprotective capacity in both studied periods, May and October, with photoinhibition rates remaining below 20%. A clear change in photoacclimation state was observed, following the seasonal change in solar radiation, with acclimation to lower irradiances in autumn being associated with higher susceptibility to photoinhibition. Also the relative importance of vertical migration and the xanthophyll cycle varied between the sampling periods. While the two processes displayed a similar role in spring/summer, vertical migration became the dominant photoprotective process in autumn. However, the contribution of the two processes to overall photoprotection



reached only ca. 20%, suggesting the participation of other photoprotective mechanisms.

Running head: Photoprotection and photoinhibition in microphytobenthos

Key index words: microphytobenthos; photoinhibition; photoprotection; xanthophyll cycle; vertical migration; non-photochemical quenching; chlorophyll fluorescence; diatoms



## INTRODUCTION

Benthic microalgae inhabiting estuarine intertidal flats are exposed to extreme and highly variable environmental conditions. Particularly during low tide, the sedimentary environment is characterized by the exposure to high levels of solar irradiance (Serôdio & Catarino 1999), including UV radiation (Waring et al. 2007, Mouget et al. 2008), extreme temperatures and salinities (Brotas et al. 2003, Rijstenbil 2005), intense rates of desiccation (Coelho et al. 2009), supersaturated oxygen concentrations (Chevalier et al. 2010), and nutrient and carbon depletion (Miles & Sundbäck 2000, Cook & Røy 2006). Being potentially damaging to the photosynthetic apparatus when acting individually, the combined effects of all these factors likely concur to the photoinhibition of photosynthesis of microphytobenthos microalgae. Of particular importance is the exposure to direct sunlight, which can result in excessive reductant pressure and in the formation of intracellular reactive oxygen species (ROS; Roncarati et al. 2008, Waring et al. 2010). High levels of ROS cause the permanent inactivation of photosystem II (PSII) protein D1, negatively impacting on photosynthetic yield and on primary productivity (Nishiyama et al. 2006).

Despite these harsh conditions, microphytobenthos of intertidal flats typically exhibit high growth rates, forming dense and diverse sedimentary biofilms, and are recognized as a major contributor to ecosystem-level carbon fixation and primary productivity (Underwood & Kromkamp 1999). Furthermore, the apparent lack of photoinhibition in microphytobenthic biofilms has been repeatedly reported (Kromkamp et al. 1998, Underwood 2002, Blanchard & Cariou-LeGall 1994, Blanchard et al. 2004, Underwood et al. 2005, Van Leeuwe et al. 2008). This success in coping with high light stress may be explained by the combined operation of two processes, the xanthophyll cycle and vertical migration, which could result in an overall particularly



83 efficient photoprotection (Serôdio et al. 2008, Perkins et al. 2010). In diatoms, the group  
84 of microalgae that typically dominate in microphytobenthos assemblages, the  
85 xanthophyll cycle has been reported to provide an exceptionally high photoprotective  
86 capacity (Lavaud 2007, Brunet & Lavaud 2010, Goss & Jakob 2010). This is  
87 particularly true for microphytobenthos *in situ* (Serôdio et al. 2005, Van Leeuwe et al.  
88 2008, Jordan et al. 2010, Chevalier et al. 2010). To this also seems to contribute the  
89 activation of the xanthophyll cycle in the dark, attributed to chlorespiratory activity,  
90 which has been considered as potentially advantageous during prolonged periods of  
91 darkness (Jakob et al. 2001, Cruz et al. 2011), a situation common in the sedimentary  
92 environment.

93         On the other hand, the negative phototactic behavior of benthic diatoms, mostly  
94 raphid pennates, under high light has long been interpreted as a form of avoidance of  
95 excessive light levels that would otherwise cause photoinhibition (Admiraal 1984,  
96 Underwood & Kromkamp 1999, Consalvey et al. 2004, Waring et al. 2007).

97         This subject has attracted substantial attention in recent years, particularly  
98 centered on the effects of vertical migration on biofilm photophysiology (Consalvey et  
99 al. 2004, Jesus et al. 2006, Waring et al. 2007, Mouget et al. 2008, Perkins et al. 2010,  
100 Cartaxana et al. 2011), and became facilitated by the introduction of a diatom motility  
101 inhibitor (Cartaxana et al. 2008). However, these studies have been focused on the  
102 response of photosynthetic activity during (Waring et al. 2007, Perkins et al. 2010) or  
103 shortly after light stress (Mouget et al. 2008), mostly through *in vivo* measurements of  
104 electron transport rate of PSII (ETR) or non-photochemical quenching (NPQ) of  
105 chlorophyll fluorescence (PAM fluorometry, see below; Table 1) (Perkins et al. 2011).  
106 Perhaps surprisingly, none of these studies has actually evaluated the efficiency of the  
107 photoprotection provided by these two processes or compared their role against



108 photoinhibition in microphytobenthos biofilms. The distinction between  
109 photoprotection and photoinhibition processes from chlorophyll fluorescence cannot be  
110 inferred from the decrease in ETR or formation of NPQ under high light, but requires  
111 the analysis of the recovery kinetics of photosynthetic activity following exposure to  
112 high light stress (Horton & Hague 1988, Walters & Horton 1991, Müller et al. 2001). In  
113 diatoms, a rapid (within minutes) component of this recovery can be attributed to the  
114 reversal of the xanthophyll cycle ( $q_E$ , or ‘energy-dependent quenching’) while  
115 photoinhibitory effects ( $q_I$ , or ‘photoinhibitory quenching’) can be quantified from a  
116 second, much slower (within hours) component (Müller et al. 2001, Lavaud 2007). The  
117  $q_T$  (state-transition related quenching) component of NPQ recovery, which shows  
118 intermediate relaxation kinetics, does not exist in diatoms (Owens, 1986). As such,  
119 questions like ‘How efficient are photoprotective processes in preventing  
120 photoinhibition in microphytobenthos biofilms?’, ‘What is the relative contribution of  
121 migration and the xanthophyll cycle for overall photoprotection?’ or ‘To what extent  
122 does photoinhibition occur in microphytobenthos?’ are mostly unanswered.

123         This study was set out to address these questions, for which a new experimental  
124 protocol was designed, based on the combination of (i) chlorophyll fluorescence  
125 imaging, to allow the simultaneous measurement of a large number of samples and  
126 experimental treatments, (ii) the use of specific inhibitors for vertical migration and for  
127 the xanthophyll cycle, to quantify the relative contribution of each process to overall  
128 photoprotection, and (iii) the analysis of the recovery kinetics of photosynthetic activity  
129 following light stress, to distinguish downregulation due to the xanthophyll cycle and  
130 photoinhibition. This approach was further used to test the influence of  
131 photoacclimation state on photoprotection capacity and susceptibility to photoinhibition  
132 in microphytobenthic biofilms inhabiting a temperate intertidal mudflat.



## MATERIALS AND METHODS

**Sampling and sample preparation.** Sediment samples were collected in the upper zone of an intertidal mudflat in the Baie de l'Aiguillon (46°15'18" N, 01°08'33" W), France, in late spring (May) and autumn (October) 2010, expected to show contrasting photoacclimation states following the seasonal variation in solar radiation (see below). The sampling site is composed of fine muddy sediments ( $< 63 \mu\text{m}$ ) where microphytobenthic biofilms are largely dominated by diatoms (Herlory et al. 2004). During low tide, samples of the surface layers of sediment (approximately the top 1 cm) were collected using a spatula. In the laboratory, the sediment was sieved through a 500- $\mu\text{m}$  mesh, to remove the mud snails *Hydrobia* sp. and other meio- and macrofauna, and was thoroughly mixed and spread in 4 cm deep plastic trays. The sediment was covered by water collected in the sampling site and left undisturbed overnight. In the next morning, at the start of the photoperiod, the slurries were again homogenized and identical portions of the resulting slurry were transferred to 24-well plates using a small spatula, filling the wells completely (ca. 3 ml). The well plates were exposed to homogeneous light field provided by two LED panels (equal contribution of red, far-red, blue and white LEDs; FloraLEDs panels, Plant Climatics, Germany) delivering a constant irradiance of  $70 \mu\text{mol quanta m}^{-2} \text{s}^{-1}$  at the sample surface, in order to induce the upward migration of microalgae and the formation of the biofilm. Daily global solar radiation were obtained from a Meteo-France weather station located approximately 9 kms southwest from the sampling site, for two-week periods preceding the sampling dates, 15-30 May and 5-20 October 2010.

**Fluorescence measurements.** Chlorophyll fluorescence was measured using an imaging-PAM fluorometer (Maxi-PAM M-series, Walz GmbH, Effeltrich, Germany).



The measuring area of the fluorometer covered each entire well plate, so that up to a total of 24 sediment samples could be monitored simultaneously. All experiments were carried out after biofilm formation. This was determined by measuring the fluorescence level  $F_s$ , taken as a proxy for surface microalgal biomass, in a replicated set of samples exposed to constant low light of  $55 \mu\text{mol quanta m}^{-2} \text{ s}^{-1}$ . Experiments were started after  $F_s$  reached a plateau following the initial rise after on the onset of the light period which typically took 2-3 hours of low light exposure. For each sample, the fluorescence signal was calculated by averaging the values of all pixels included in an area of ca.  $63.6 \text{ mm}^2$  (area of interest), which corresponded to ca. 1500 pixels, centered inside each well. This area is smaller than the total area of each well ( $95.0 \text{ mm}^2$ ), the difference being due to the exclusion of the edge of each sample, often not representative of the rest of the biofilm. To minimize sample heating during prolonged exposure to high light, the experiments were carried out in a temperature-controlled room, at  $20^\circ\text{C}$ , and the fluorometer Perspex hood was maintained open at all times.

**Photoacclimation: light-response curves.** The photoacclimation state of the samples was characterized by measuring light-response curves of ETR and of NPQ in the two sampling periods. Light-response curves were generated by sequentially exposing the samples to 7 levels of actinic light, up to  $700 \mu\text{mol quanta m}^{-2} \text{ s}^{-1}$ . Samples were exposed to each light level for 3 min (a period previously confirmed allowing for reaching a steady-state), after which a saturation pulse was applied and fluorescence levels  $F_s$  and  $F_m'$  were recorded. Six replicated measurements (on six different wells) were made for each light level. For each irradiance level,  $E$ , the relative ETR was calculated from the product of  $E$  and the PSII effective quantum yield,  $\Delta F/F_m'$  (Genty et al. 1989):



$$ETR = E \frac{F'_m - F'_s}{F'_m} \quad (1)$$

ETR vs  $E$  curves were quantitatively described by fitting the model of Eilers & Peeters (1988), and by estimating the parameters  $\alpha$  (the initial slope of the curve),  $ETR_m$  (maximum ETR) and  $E_k$  (the light-saturation, or photoacclimation, parameter):

$$ETR(E) = \frac{E}{a E^2 + b E + c} \quad (2)$$

where

$$\alpha = \frac{1}{c}, \quad ETR_m = \frac{1}{b + \sqrt{ac}} \quad \text{and} \quad E_k = \frac{c}{b + \sqrt{ac}} \quad (3)$$

Due to the unavoidable confounding effects of vertical migration on the measurement of  $F_m$ , NPQ was calculated using the adapted index, based on the relative difference between the maximum fluorescence measured during the construction of the light curve,  $F'_{m,m}$ , and upon exposure to light,  $F'_m$  (Serôdio et al. 2005):

$$NPQ = \frac{F'_{m,m} - F'_m}{F'_m} \quad (4)$$

NPQ vs  $E$  curves were described by fitting the model of Serôdio & Lavaud (2011), and by estimating the parameters  $NPQ_m$  (maximum NPQ),  $E_{50}$  (irradiance corresponding to half of  $NPQ_m$ ) and  $n$  (sigmoidicity parameter):



$$NPQ(E) = NPQ_m \frac{E^n}{E_{50}^n + E^n} \quad (5)$$

These models were fitted using a procedure written in MS Visual Basic and based on MS Excel Solver. Model parameters were estimated iteratively by minimizing a least-squares function, forward differencing, and the default quasi-Newton search method. The model was fitted to individual light-response curves. Estimates of model parameters were compared using the Student's *t*-test. The standard errors of the parameter estimates were calculated following Ritchie (2008).

**Photoprotection vs photoinhibition: light stress-recovery experiments.** The photoprotection capacity of microphytobenthos biofilms was estimated by quantifying the recovery of  $\Delta F/F_m'$  following a prolonged exposure to supersaturating irradiance. Three replicates were sequentially exposed to: (i) low light level of  $55 \mu\text{mol quanta m}^{-2} \text{s}^{-1}$ , for a minimum of 15 min, to ensure full light-activation of the photosynthetic apparatus and to determine pre-stress reference levels of  $\Delta F/F_m'$ ; (ii) supersaturating light level of  $1200 \mu\text{mol quanta m}^{-2} \text{s}^{-1}$  for 3 hrs, to potentially induce photoinhibitory effects; (iii) low light ( $55 \mu\text{mol quanta m}^{-2} \text{s}^{-1}$ ) for a minimum of 15 min to record the recovery kinetics. During the whole experiment,  $\Delta F/F_m'$  was measured by applying saturating pulses every 90 s. The recovery of  $\Delta F/F_m'$  upon the return to low light conditions was described by fitting an exponential function, adapted from a first-order kinetics model derived for describing the kinetics of NPQ (Olaizola & Yamamoto 1994, Serôdio et al. 2005):

$$\Delta F / F_m'(t) = \Delta F / F_{m,rec}' + \left[ \Delta F / F_m'(0) - \Delta F / F_{m,rec}' \right] e^{-kt} \quad (6)$$



where  $t$  is the time during recovery,  $\Delta F/F_m'(0)$  and  $\Delta F/F_m'_{rec}$  represent the PSII quantum yield levels at the start of the recovery period and after full recovery (associated to  $q_E$ ), and  $k$  is the rate constant of  $\Delta F/F_m'$  recovery. The values of  $\Delta F/F_m'$  estimated by the model for  $t = 10.5$  min, expressed as a percentage of the pre-stress levels, were used for estimating the effective photoprotective capacity of the biofilm. The remaining relative difference between pre- and post-stress levels of  $\Delta F/F_m'$  was used as an estimate of the photoinhibitory effects imposed by high light.

The photoprotective roles of vertical migration and of the xanthophyll cycle were studied by applying specific inhibitors of the two processes. Vertical migration was inhibited by the diatom motility inhibitor Latrunculin (Lat) A, shown to effectively inhibit cell motility without causing appreciable effects on the photosynthetic activity (Cartaxana et al. 2008). To inhibit the activity of the xanthophyll cycle, the inhibitor of the diadinoxanthin de-epoxidase (DDE) dithiothreitol (DTT) was used. DTT is commonly used to inhibit the conversion of the pigment diadinoxanthin (DD) into the photoprotective form diatoxanthin (DT) (Lavaud et al. 2002a). DTT was applied in combination with Lat A, in order to ensure that the cells having the xanthophyll cycle inhibited remained exposed to high light.

The contribution of vertical migration to overall photoprotection capacity of the biofilm was estimated by the difference between the levels of  $\Delta F/F_m'$  recovery in control (free moving cells) and Lat A-treated (vertical migration inhibited) samples. The contribution of the xanthophyll cycle was estimated by comparing the levels of  $\Delta F/F_m'$  recovery in the samples treated with Lat A (only vertical migration inhibited) and in those treated with both Lat A and DTT (both vertical migration and the xanthophyll cycle inhibited). The inhibitor solutions were added after biofilm was fully formed, in a total of 200  $\mu$ L for both the Lat A and the Lat A + DTT solutions. The same volume of



filtered seawater was added to the control samples. The solutions were added carefully to minimize biofilm disturbance, by pipetting small volumes onto the sediment surface. A minimum of 30 min was given for the inhibitors to diffuse and for the biofilms to stabilize before measurements were started.

**Inhibitor preparation and effective dosage.** Solutions of Lat A of different concentrations, ranging from 5 to 15  $\mu\text{M}$ , were prepared from a concentrated solution (1 mM) prepared from dissolving purified Lat A (Sigma-Aldrich) in dimethylsulfoxide. The minimum effective dosage of Lat A to induce inhibition of vertical migration was determined following Cartaxana & Serôdio (2008). Samples treated with different concentrations of Lat A (final volume, 200  $\mu\text{L}$ ) were darkened close to the time expected for tidal flood, known to induce a rapid downward migration. The degree of migration inhibition was estimated from the decrease in surface biomass following darkening, as estimated from dark-adapted fluorescence level,  $F_o$ . Three replicated samples were tested for each Lat A concentration.

DTT (BDH-Prolabo) was prepared fresh as in Lavaud et al. (2002a). A stock solution of 300 mM (in ethanol) was diluted in filtered seawater to prepare working solutions of concentrations ranging from 3.3 to 15 mM. The minimum effective dosage of DTT was determined by measuring NPQ development upon exposure to 400  $\mu\text{mol quanta m}^{-2} \text{ s}^{-1}$  for 30 min in samples treated with increasing concentration of DTT (final volume, 200  $\mu\text{L}$ ). Three replicated samples were tested for each DTT concentration. For the light stress experiments, samples were treated with 200  $\mu\text{L}$  of a combined solution of Lat A and DTT, prepared using the concentration of each inhibitor determined from the effective dosage tests (see Results).

**Taxonomic composition.** In one of the trays, microalgae were collected by covering the sediment with two layers of a 100  $\mu\text{m}$ -mesh. The trays were exposed to



low indirect natural light from a north facing window ( $< 200 \mu\text{mol quanta m}^{-2} \text{ s}^{-1}$ ) during the day following the sampling. The upper mesh was removed at the time of middle emersion period and it was washed with filtered ( $0.2 \mu\text{m}$ ) natural sea water. The samples were fixed in Lugol and preserved at  $4^{\circ}\text{C}$  until their analysis. Diatom species were identified and counted using definitive mounts in Naphrax after cleaning the cells by cremation (2 h,  $450^{\circ}\text{C}$ ) (Méléder et al. 2007). Taxonomic determination was performed by microscope on the basis of morphological criteria. A total of ca. 300 diatom frustules were counted to determine specific abundances.

## RESULTS

### Taxonomic composition

In both sampling periods, the microphytobenthic assemblages were dominated by long biraphid diatoms (length  $> 30 \mu\text{m}$ ). In May, the assemblages were mainly dominated by *Navicula cf. spartinentensis* (61%,  $n = 350$ ). *Staurophora salina* represented less than 20% of the assemblages but this species was two times longer than *N. cf. spartinentensis* (22  $\mu\text{m}$  and 44  $\mu\text{m}$  long, respectively). In October, the assemblages were co-dominated by *Plagiotropis seriata* (22%,  $n = 335$ ) and *Staurophora salina* (19%); the size of *P. seriata* (190  $\mu\text{m}$  long) was four times the one of *S. salina* one (44  $\mu\text{m}$  long) strengthening its dominance in terms of biovolume. A third species, *Pleurosigma strigosum* (300  $\mu\text{m}$  length) represented more than 10% of the assemblage abundance.

### Photoacclimation



Significant differences were found between the light-response of ETR measured in May and October. In comparison with the ETR vs  $E$  curves measured in May, the ones measured in October presented significantly higher values of  $\alpha$  (+26.7%,  $t$ -test,  $p < 0.001$ ) and lower values of  $ETR_m$  (-41.5%,  $t$ -test,  $p < 0.001$ ) (Fig. 1A). As a consequence, the photoacclimation parameter  $E_k$  was significantly lower in October than in May (-53.5%;  $t$ -test,  $p < 0.001$ ). Regarding NPQ, significant differences were found between the light-response curves measured in the two periods (Fig. 1B). NPQ vs  $E$  curves measured in May reached lower levels within the range of applied irradiances (on average, 2.19 and 3.25 at  $700 \mu\text{mol quanta m}^{-2} \text{s}^{-1}$ , in May and October, respectively), although the values of  $NPQ_m$  were not significantly different ( $t$ -test,  $p = 0.425$ ). The light-response curves were more sigmoid in May than in October ( $t$ -test,  $p = 0.001$ ), the largest differences being found regarding the light level required for induction of NPQ, indicated by the parameter  $E_{50}$ , which was significantly lower in October than in May (-38.5%;  $t$ -test,  $p = 0.003$ ).

The light conditions in the region of the sampling area varied greatly between the two-week periods preceding the sampling periods, with global solar radiation reaching a daily average of  $2369 \text{ J cm}^{-2}$  in May, more than double the value observed in October,  $1008 \text{ J cm}^{-2}$ .

### **Inhibitor dosage**

Vertical migration was strongly inhibited for most of the Lat A concentrations tested, with an inhibition level above 75% being obtained with only  $5 \mu\text{M}$  (Fig. 2). The inhibitory response to the increase in Lat A concentration presented a clear saturation-like pattern, with the increase from 10 to  $15 \mu\text{M}$  resulting in an increase in inhibition of



only 8.5%. Considering that 10  $\mu$ M was enough to inhibit vertical migration by more than 90%, and the small increase obtained by applying the higher concentrations, solutions of 10  $\mu$ M Lat A were used in all experiments.

The response of NPQ to the increase in DTT also showed a saturation-like pattern, characterized by a strong decrease for concentrations up to 5 mM, and a virtually constancy for concentrations above this value (NPQ decreased by 19% between 5 and 15 mM; Fig. 3). However, even when the highest DTT concentration was applied, NPQ was never completely eliminated, remaining above 1.0. In all further experiments, a concentration of DTT of 10 mM was used.

### **Light stress exposure and recovery**

Figure 4 exemplifies the variation of  $\Delta F/F_m'$  during a light stress-recovery experiment. On control samples, exposure to high light induced an immediate and marked decrease in  $\Delta F/F_m'$  from ca. 0.63 to values slightly below 0.1 (Fig. 4).  $\Delta F/F_m'$  further decreased to values close to zero during the first 15 min of exposure, after which it gradually recovered, stabilizing at values around 0.1 after 90 min and until the end of the high light period. On inhibitor-treated samples,  $\Delta F/F_m'$  also decreased to values close to zero upon the start of high light exposure, but, as opposed to control samples, never showed any appreciable recovery, remaining below 0.05 (Fig. 4). However,  $\Delta F/F_m'$  levels were usually higher in Lat A-treated samples than in those treated with both inhibitors (Figs. 4, 5). Following the transition to low light, a clear recovery response was observed for all samples, with  $\Delta F/F_m'$  reaching in all cases over 60% of initial values after 15 min. Treatment with Lat A effectively inhibited vertical migration during the whole experiment, as indicated by the small variation in  $F_s$  in Lat A-treated



samples (on average, -12.1% for samples treated with Lat A and Lat A+DTT) as compared with the controls (-43.5%; Fig. 6). The effects of inhibitors were particularly evident during recovery under low light, during which  $\Delta F/F_m'$  followed the negative exponential pattern described by Eq. (6), the fit of which was very good in all cases ( $r^2 > 0.91$ ; Fig. 7). Control samples recovered more rapidly than those treated with inhibitors, so that after 3 min after return to low light,  $\Delta F/F_m'$  of non-inhibited samples was over 70% and 60% higher than on samples treated with Lat A in May and October, respectively. In both periods these differences were gradually reduced during exposure to low light, but after 10.5 min the percentage of recovery was significantly different among treatments and sampling periods (two-way ANOVA,  $p < 0.001$  for both factors). In both May and October, the recovery of  $\Delta F/F_m'$  was higher in the controls than in the Lat A-treated samples (Control vs Lat A; Tukey's post-hoc test,  $p = 0.043$  and  $p = 0.010$ , respectively), which was in turn higher than in samples treated with Lat A and DTT (Lat A vs Lat A+DTT; Tukey's post-hoc test,  $p = 0.042$  and  $p = 0.030$ , respectively). The percentage of recovery was in all cases significantly higher in May than in October (Tukey's post-hoc test,  $p < 0.05$ ), with the exception of samples treated with both inhibitors (Tukey's post-hoc test,  $p = 0.107$ ).

### **Photoprotection efficiency and extent of photoinhibition**

Depending on the species, the full recovery of the xanthophyll cycle after a transition from high to low light mainly occurs after 6 min to 15 min (Goss et al. 2006, Lepetit & Lavaud, pers. obs.). Considering the intermediate period of 10.5 min, the recovery of  $\Delta F/F_m'$  at this time was used as an estimate of the photoprotection capacity and to calculate the extent of photoinhibition occurred. The results indicate that the



microphytobenthos biofilms had a large photoprotective capacity in both periods, with a correspondingly low percentage of photoinhibition below 25%, although higher in May than in October (87.7 and 78.0%; Fig. 8, Table 2). From the reduction in the photoprotection capacity measured in samples treated with inhibitors, the contribution of vertical migration and of the xanthophyll cycle to overall photoprotection were estimated to reach a combined value only slightly above 20% (Table 2). While in May the two processes had a comparable contribution to photoprotection, the relative importance of the xanthophyll cycle was reduced to 7.2% in October.

## DISCUSSION

### Photoacclimation and susceptibility to photoinhibition

Comparatively to May, samples collected in October appeared acclimated to lower light levels, showing the pattern typically associated to ‘shade-acclimation’: a combination of higher values of  $\alpha$  and of lower values of  $ETR_m$ , resulting in lower values of  $E_k$ , usually taken as an indication of photosynthesis saturating at lower irradiances. This change in photoacclimation state between May and October was consistent with the observed seasonal change in solar light conditions preceding the two sampling periods (i.e. global solar radiation more than two times higher in May than in October). These results also generally confirmed previous observations on the seasonal variability of microphytobenthos photosynthetic performance, showing patterns of acclimation to higher light levels during spring/summer and to lower levels in autumn/winter (Blanchard et al. 1997, Migné et al. 2004, Serôdio et al. 2006). They were also



consistent with the photoacclimation response of benthic diatoms grown in culture exposed to low and high-light regimes (Perkins et al. 2006, Schumann et al. 2007, Cruz & Serôdio 2008). Increases of  $\alpha$ , as the observed from May to October, are commonly attributed to an increase in the cellular content of light-harvesting pigments, increasing the fraction of incident light that is intercepted and absorbed for photosynthesis; decreases in  $ETR_m$  are typically associated with the decrease of the activity of the electron transport chain or the Calvin cycle, limiting factors of light-saturated photosynthesis (Henley 1993, MacIntyre et al. 2002, Behrenfeld et al. 2004).

A change in light response was also noticeable regarding NPQ, with the samples collected in October showing NPQ activation starting at lower light levels (lower  $E_{50}$ ) and higher values of NPQ for most irradiances (higher  $NPQ_m$ ). As with ETR, the observed variation in the NPQ vs  $E$  curves was consistent with the previously reported for microphytobenthos (Serôdio et al. 2006) or for benthic diatoms acclimated to different light regimes (Cruz & Serôdio 2008).

However, while changes in the light-response of ETR may be interpreted and related to underlying physiological processes in a relatively straightforward manner, the physiological meaning of changes in NPQ levels is more difficult to ascertain. This is because the two components of NPQ,  $q_E$  (photoprotection) and  $q_I$  (photoinhibition) can only be distinguished through the analysis of the recovery kinetics after exposure to high light, but not from NPQ light curves. In this study, the light stress-recovery experiments allowed to conclude that the observed change in the NPQ light-response curves was due to a decrease in the  $q_E$  component and a concomitant increase in the  $q_I$  component. In the absence of information from NPQ recovery kinetics, similar increases in NPQ vs  $E$  curves in autumn/winter periods have been, perhaps wrongly,



interpreted as being due to an increase in photoprotective capacity (Serôdio et al. 2005, 2006).

Furthermore, the results from the light stress-recovery experiments revealed an association between photoacclimation status and photoprotection efficiency, not shown before for these communities. Whatever the cause (see below), the acclimation to high light levels in summer was associated to a high photoprotection capacity and the low light-acclimation in autumn to a general loss in photoprotection and a higher susceptibility to photoinhibition.

### **Photoprotection vs photoinhibition**

A central finding of this study is that photoinhibition was in all cases considerably low (ca. 20%), indicating photoprotection to be particularly efficient in the studied microphytobenthos biofilms. Despite the general view that these assemblages are largely immune to photoinhibition (Blanchard et al. 2004, Waring et al. 2007, Mouget et al. 2008), this process has been shown to occur under *in situ* conditions (Serôdio et al. 2008). Curiously, the rates of photoinhibition estimated in the cited study, reaching up to ca. 18%, are similar to the values here reported, despite the fact that they were estimated from hysteresis patterns observed during entire low tide exposure periods. The results of the present study therefore confirm that the photoprotective mechanisms available to benthic diatoms are not completely efficient in preventing some degree of photoinhibitory damage. However, it should be stressed the difficulty in comparing the measured rates of photoinhibition with results published for other habitats, or for other estuarine primary producers such as phytoplankton, seagrasses or macroalgae. Apart from the light history and the species-specific



differences, the extent of photoinhibition is directly related to light dosage, determined by light intensity and duration of exposure, both largely variable amongst the different experimental protocols used in different laboratory and field studies.

A number of unaccounted factors may have contributed for the measured low values of  $q_I$ . Firstly, the well-known effect of depth-integration of subsurface fluorescence (Forster & Kromkamp 2004, Serôdio 2004). This effect is caused by the fact that only the cells at or near the surface are actually exposed to measured levels of high light, and that the fluorescence signal measured at the surface also accounts for cells positioned deeper in the photic zone and exposed to lower light levels. The expected effect is a light-dependent overestimation of biofilm-level  $\Delta F/F_m'$  relatively to the inherent, physiological values of the cells at the surface, which is then expected to cause a systematic overestimation of  $q_E$  and the underestimation of  $q_I$  (Serôdio 2004). However, besides this static effect, also dynamic effects can be expected. During prolonged exposure to high light, the downward migration of microalgae to less illuminated layers is likely to induce a gradual increase of  $\Delta F/F_m'$  (as measured at the surface), independently of any photophysiological changes, thus causing the overestimation of  $q_E$ . It is also conceivable that these types of effects may affect the measurement of  $\Delta F/F_m'$  during the recovery under low light, due to upward migration as a response to the decrease in incident irradiance. This, however, seems less likely due to the relatively short time of this period and to the fact that a transition from high to low light is a weaker stimulus for vertical migration, especially if coinciding with the end of the low tide period (Coelho et al. 2011).

A second factor that might explain the low values of  $q_I$  is the light doses applied during the light stress-recovery experiments in the laboratory. Because these (3 hrs,  $1200 \mu\text{mol quanta m}^{-2} \text{ s}^{-1}$ ) were likely lower than the ones received during a typical



period of exposure at low tide (up to 8-10 hrs, 1500-2000  $\mu\text{mol quanta m}^{-2} \text{ s}^{-1}$ ), larger, but still ecologically relevant, light doses could have been applied which would likely induce larger cumulative photoinhibitory effects. The light exposure conditions applied in this study, both regarding light intensity and duration, resulted from a compromise between inducing measurable effects, instrument limitations (maximum PAR irradiance provided by the imaging fluorometer) and minimizing uncontrollable experimental conditions (excessive sample heating and desiccation caused by the fluorometer LED panel). Despite these limitations, mostly instrument-related, the laboratory experimental approach used in this study has the advantage over studies carried out under *in situ* conditions (e.g. Serôdio et al. 2008; Perkins et al. 2010) of allowing applying controlled and reproducible conditions, making it possible to directly compare the migratory and physiological responses of samples collected in different places and occasions.

The estimation of  $q_E$  and  $q_I$  is also directly affected by the type of analysis made on the recovery kinetics in order to distinguish the two components of NPQ. For higher plants,  $q_E$  and  $q_I$  are distinguished on the basis of the recovery rate of  $F_v/F_m$ , typically 10-15 min, assumed to correspond to the full reversal of the xanthophyll cycle (Horton & Hague 1988, Ruban & Horton 1995). Following the common practice for the distinction of  $q_E$  and  $q_I$ , in this study these two components of NPQ were estimated based on a relaxation time of the xanthophyll cycle of 10.5 min. However, to evaluate the possible effects of considering different times for the reversal of the xanthophyll cycle on the relative magnitude of  $q_E$  and  $q_I$ , a sensitivity analysis was performed, consisting on the re-calculation of these estimates when considering 6 and 15 min, values matching the range of relaxation times of the xanthophyll cycle expectable for diatoms (Gross et al. 2006, Lepetit & Lavaud, pers. obs.). The use of these different recovery periods did not alter significantly the general findings of the study, including



high levels of recovery and low photoinhibition rates, the increase in photoinhibition levels from May to October, and a relatively low (< 30%) combined contribution of vertical migration and xanthophyll cycle to overall photoprotection (Table 2). Nonetheless, this analysis shows some effects, although largely expected from the asymptotic pattern of  $\Delta F/F_m'$  recovery during the considered period: the use of a shorter period resulted in the estimation of lower rates of recovery, leading to a likely overestimation of photoinhibition rates; conversely, longer periods resulted in larger rates of recovery and probably overestimated levels of photoprotection (Table 2). Moreover, due to the different relaxation patterns of samples exposed to different treatments, the evaluation of the relative importance of vertical migration and the xanthophyll cycle was also affected by the time period considered, with shorter and longer recovery periods resulting in a higher apparent contribution of vertical migration and of the xanthophyll cycle, respectively. These effects, however, did not affect substantially the overall pattern of variation of the role of the two photoprotective processes between the two sampling periods.

Recently, more sophisticated methods, based on the mathematical modeling and deconvolution of the recovery curve, were proposed to trace the recovery of each individual component of NPQ (Roháček 2010). This method could not be applied in this study because of the particularities of the xanthophyll cycle in diatoms, which may not verify the assumptions of the method. Firstly, the lack of  $q_T$  (the state-transition quenching) in diatoms (Owens 1986, Lavaud 2007, Goss & Jakob 2010), which called for the modification of this model to a two-component NPQ. Secondly, the impossibility of using changes in  $F_v/F_m$  in biofilms as an indication of photoinhibition, as this requires the darkening of the samples, known to induce changes in  $F_m$  levels due to vertical migration. Furthermore, in benthic diatoms, dark adaptation often causes the



$F_m$  level to decrease to values below  $F_m'$  levels measured under low light (Serôdio et al. 2006). These reasons also prevented the use of other recently proposed methods to quantify the components of NPQ (Ahn et al. 2009, Guadagno et al. 2010).

The formation of DT in the dark and thus anoxic subsurface layers of the sediment, known to occur in diatoms (Jakob et al. 2001), and especially in benthic assemblages (Serôdio et al. 2006), is a likely explanation for the apparent impossibility to completely eliminate NPQ by applying the xanthophyll cycle inhibitor DTT (Fig. 3). The DT thus formed would remain present despite the treatment with DTT, which prevents new conversion of DD to DT, but does not induce the reversed reaction. Upon exposure to high light, the oxygenation of DT-rich subsurface layers would allow for the observed rise in NPQ, as the formation of NPQ from DT is known to be inhibited by anoxia (Cruz et al. 2011).

#### **Photoprotection: vertical migration vs xanthophyll cycle**

The use of specific inhibitors for vertical migration and for the operation of the xanthophyll cycle allowed estimating the relative contribution of each of these processes to overall photoprotection of the biofilm. The results showed a change with season and photoacclimation state of their relative importance. While in May the two processes seemed to contribute similarly to biofilm photoprotection, the loss of photoprotection capacity from May to October was associated to a decrease in the contribution of the xanthophyll cycle, so that vertical migration became the dominant photoprotective process. The observed change in the species composition of the microphytobenthic assemblage may explain this difference as the activity of the xanthophyll cycle can differ from a species to another (Lavaud et al. 2004, Goss et al.



2006). It may be also hypothesized that this difference is related to the decrease in rates of enzymatic conversion between DD and DT associated to photoacclimation or due to acclimation to lower temperatures (Van Leeuwe et al. 2008), an effect that is also species-related (Salleh & McMinn, 2011). Nevertheless, these results indicate that behavioral photoprotection seems able to maintain the overall photoprotection capacity, compensating for the decrease in the contribution of the xanthophyll cycle during the winter season.

The change in species composition, involving a dominance of larger cells in October, could also have affected the migratory response of the assemblages to high light. However, although some studies have shown a relation between migratory cell size and migratory behaviour in sediments (Hay et al. 1993, Underwood et al. 2005), there is no evidence that cell size is an important factor regarding the migratory response to light stress.

Vertical migration and the xanthophyll cycle have been considered as the main photoprotective mechanisms in microphytobenthos biofilms (Serôdio et al. 2005, Jesus et al. 2006, Mouget et al. 2008, Serôdio et al. 2008; Perkins et al. 2010). A perhaps surprising result of this study is the relative low contribution of these two processes to global photoprotection. This calls for the potential role of other processes responsible for the observed low rates of photoinhibition. Likely candidates include the cyclic electron flow around PSII (Lavaud et al. 2002b, 2007), the efficient scavenging of reactive oxygen species (Roncarati et al. 2008, Waring et al. 2010) or high turnover rates of the PSII protein D1 (Wu et al. 2011).

#### **Use of inhibitors on microphytobenthic biofilms**



An aim of this study was the introduction of a new experimental protocol to estimate photoprotection efficiency and the extent of photoinhibition in microphytobenthos biofilms. This involved the combination of: (i) the use of specific inhibitors for different photoprotective processes, applied alone and in combination with each other, allowing the estimation of the relative contribution of each process to overall photoprotection, and (ii) the use of imaging fluorometry on replicated samples in well plates, taking advantage of the self-forming nature of microphytobenthos biofilms from homogenized sediments, which allowed for adequate replication and low variability between replicates, and for the simultaneous testing of different treatments.

Some potential pitfalls exist regarding the use of inhibitors on biofilms and the interpretation of results. Firstly, it must be noted that when comparing controls (no inhibitor added) with Lat A-treated samples, it is likely that the differences in fluorescence parameters observed over time may not be attributed only to changes in cell physiological conditions but also to changes in cell composition in the upper layers of the sediment. This is because in the controls, as opposed to Lat A-treated samples, cells initially at the surface likely migrated down into layers below the photic zone, therefore changing the contribution to the fluorescence signal measured at the surface. As a consequence, any observed differences are expected to represent mainly changes at the biofilm (i.e., community)-level, and not only changes in the physiology of individual cells. This also explains the need to combine Lat A and DTT if the effect of inhibiting the xanthophyll cycle is to be evaluated in the same microalgal assemblage. By adding DTT to samples treated with Lat A, it is ensured that the same cells remain in the photic zone of the sediment and that measured changes in fluorescence are due to changes in their physiological status and not to changes in community composition. If only DTT is applied (Perkins et al. 2010), only biofilm-level effects can be evaluated, as



601 many cells will likely respond to high light by migrating downward and become  
602 unobservable (Oxborough et al. 2000).

603



*Acknowledgements.* We thank Dr. Céline Vincent for providing solar radiation data.  
This study was supported by FCT – Fundação para a Ciência e a Tecnologia, through  
grants SFRH/BSAB/962/2009 (J. Serôdio), SFRH/BD/44860/2008 (J. Ezequiel), and  
project MigROS (PTDC/MAR/112473/2009), and by the CNRS – Centre National de la  
Recherche Scientifique (‘chercheurs invités’ program, J. Serôdio and J. Lavaud), the  
region Charente-Maritime/CG17 (A. Barnett Ph.D. grant), and the French consortium  
CPER-Littoral., . We thank two anonymous reviewers for critical comments on the  
manuscript.



## LITERATURE CITED

- Admiraal, W (1984) The ecology of estuarine sediment-inhabiting diatoms. *Progr Phycol Res* 3:269-322
- Ahn, TK, Avenson, TJ, Peers, G, Li, Z, Dall'Osto, L, Bassi, R, Niyogi, KK, Fleming, GR (2009) Investigating energy partitioning during photosynthesis using an expanded quantum yield convention. *Chem Phys* 357:151-158
- Behrenfeld MJ, Prasil O, Babin M, Bruyant, F (2004) In search of a physiological basis for covariations in light-limited and light-saturated photosynthesis. *J Phycol* 40:4-25
- Blanchard GF, Guarini J-M, Dang C, Richard P (2004) Characterizing and quantifying photoinhibition in intertidal microphytobenthos. *J Phycol* 40:692-696
- Blanchard GF, Cariou-Le Gall V (1994) Photosynthetic characteristics of microphytobenthos in Marennes-Oléron Bay, France: Preliminary results. *J Exp Mar Biol Ecol* 182:1-14
- Blanchard GF, Guarini JM, Gros P, Richard P (1997) Seasonal effect on the the relationship between the photosynthetic capacity of intertidal microphytobenthos and temperature. *J Phycol* 33:723-728
- Brotas V, Risgaard-Petersen N, Ottossen L, Serôdio J, Ribeiro L, Dalsgaard T (2003) *In situ* measurement of photosynthetic activity and respiration of intertidal benthic microalgal communities undergoing vertical migration. *Ophelia* 57:13-26
- Cartaxana P, Ruivo M, Hubas C, Davidson I, Serôdio J, Jesus B (2011) Physiological versus behavioural photoprotection in intertidal epipellic and epipsamic benthic diatom communities. *J Exp Mar Biol Ecol* 405:120-127



- Cartaxana P, Serôdio J (2008) Inhibiting diatom motility: a new tool for the study of the photophysiology of intertidal microphytobenthic biofilms. *Limnol Oceanogr Meth* 6:466-476
- Cartaxana P, Brotas V, Serôdio J (2008) Effects of two motility inhibitors on the photosynthetic activity of the diatoms *Cylindrotheca closterium* and *Pleurosigma angulatum*. *Diatom Res* 23:65-74
- Chevalier EM, Gévaert F, Créach A (2010) In situ photosynthetic activity and xanthophylls cycle development of undisturbed microphytobenthos in an intertidal mudflat. *J Exp Mar Biol Ecol* 385:44-49
- Coelho H, Vieira S, Serôdio J (2009) Effects of desiccation on the photosynthetic activity of intertidal microphytobenthos biofilms as studied by optical methods. *J Exp Mar Biol Ecol* 381:98-104
- Coelho H, Vieira S, Serôdio J (2011) Endogenous versus environmental control of vertical migration by intertidal benthic microalgae. *Eur J Phycol* 46:271-281
- Consalvey M, Paterson DM, Underwood GJC (2004) The ups and downs of life in a benthic biofilm: migration of benthic diatoms. *Diatom Res* 19:181-202
- Cook PLM, Røy H (2006) Advective relief of CO<sub>2</sub> limitation in microphytobenthos in highly productive sandy sediments. *Limnol Oceanogr* 51:1594-1601
- Cruz S, Goss R, Wilhelm C, Leegood R, Horton P, Jakob T (2011) Impact of chlororespiration on non-photochemical quenching of chlorophyll fluorescence and on the regulation of the diadinoxanthin cycle in the diatom *Thalassiosira pseudonana*. *J Exp Bot* 62:509-519
- Cruz S, Serôdio J (2008) Relationship of rapid light curves of variable fluorescence to photoacclimation and non-photochemical quenching in a benthic diatom. *Aquat Bot* 88:256-264



Eilers PHC, Peeters JCH (1988) A model for the relationship between light intensity and the rate of photosynthesis in phytoplankton. *Ecol Model* 42:199-215

Forster RM, Kromkamp JC (2004) Modelling the effects of chlorophyll fluorescence from subsurface layers on photosynthetic efficiency measurements in microphytobenthic algae. *Mar Ecol Prog Ser* 284:9-22

Genty B, Briantais J-M, Baker, NR (1989) The relationship between the quantum yield of photosynthetic electron transport and quenching of chlorophyll fluorescence. *Biochim Biophys Acta* 990:87-92

Goss R, Pinto AE, Wilhelm C, Richter M (2006) The importance of a highly active and  $\Delta$ pH-regulated diatoxanthin epoxidase for the regulation of the PS II antenna function in diadinoxanthin containing algae. *J Plant Physiol* 163:1008-1021

Goss R, Jakob T (2010) Regulation and function of xanthophyll cycle-dependent photoprotection in algae. *Photosynth Res* 106:103-122

Grouneva I, Jakob T, Wilhelm C, Goss, R (2008) A new multicomponent NPQ mechanism in the diatom *Cyclotella meneghiniana*. *Plant Cell Physiol* 49:1217-25

Guadagno CR, Virzo De Santo A, D'Ambrosio N (2010) A revised energy partitioning approach to assess the yields of non-photochemical quenching components. *Biochim Biophys Acta* 1797:525-30

Hay SI, Maitland TC, Paterson DM (1993) The speed of diatom migration through natural and artificial substrata. *Diatom Res* 8:371-384

Henley, WJ (1993) Measurement and interpretation of photosynthetic light-response curves in algae in the context of photoinhibition and diel changes. *J Phycol* 29:729-739



685 Herlory O, Guarini J-M, Richard P, Blanchard G (2004) Microstructure of  
 686 microphytobenthic biofilm and its spatio-temporal dynamics in an intertidal  
 687 mudflat (Aiguillon Bay, France). *Mar Ecol Prog Ser* 282:33-44

688 Horton P, Hague A (1988) Studies on the induction of chlorophyll fluorescence in  
 689 isolated barley protoplasts. 4. Resolution of non-photochemical quenching.  
 690 *Biochim Biophys Acta* 932:107-115

691 Jakob T, Goss R, Wilhelm, C (2001) Unusual pH-dependence of diadinoxanthin de-  
 692 epoxidase activation causes chlororespiratory induced accumulation of  
 693 diatinoxanthin in the diatom *Phaeodactylum tricornutum*. *J Plant Physiol* 158:383-  
 694 390

695 Jordan L, McMinn A, Thompson P (2010) Diurnal changes of photoadaptive pigments  
 696 in microphytobenthos. *J. Mar Biol Ass UK* 90:1025-1032

697 Jesus B, Perkins RG, Consalvey M, Brotas V, Paterson DM (2006) Effects of vertical  
 698 migrations by benthic microalgae on fluorescence measurements of  
 699 photophysiology. *Mar Ecol Prog Ser* 315:55-66

700 Kromkamp J, Barranguet C, Peene J (1998) Determination of microphytobenthos PSII  
 701 quantum efficiency and photosynthetic activity by means of variable chlorophyll  
 702 fluorescence. *Mar Ecol Prog Ser* 162: 45-55

703 Lavaud J, Gorkom HJV, Etienne A-L (2002b) Photosystem II electron transfer cycle  
 704 and chlororespiration in planktonic diatoms. *Photosynth Res* 74:51-59

705 Lavaud J, Rousseau B, Etienne A-L (2002a) In diatoms, a transthylakoidal proton  
 706 gradient alone is not sufficient to induce a non-photochemical fluorescence  
 707 quenching. *FEBS Lett* 523:163-166



708 Lavaud J, Rousseau B, Etienne A-L (2004) General features of photoprotection by  
 709 energy dissipation in planktonic diatoms (Bacillariophyceae). *J Phycol* 40:130-  
 710 137

711 Lavaud L, Kroth PG (2006) In diatoms, the transthylakoidal proton gradient regulates  
 712 the photoprotective non-photochemical fluorescence quenching beyond its  
 713 control on the xanthophyll cycle. *Plant Cell Physiol* 47:1010-1016

714 Lavaud, J (2007) Fast Regulation of Photosynthesis in Diatoms: Mechanisms, Evolution  
 715 and Ecophysiology. *Funct Plant Sci Biotechnol* 1:267-287

716 Lavaud J, Rousseau B, Etienne AL (2004) General features of photoprotection by  
 717 energy dissipation in planktonic diatoms (Bacillariophyceae). *J Phycol* 40:130-  
 718 137

719 Li Z, Wakao S, Fischer BB, Niyogi KK (2009) Sensing and responding to excess light.  
 720 *Ann Rev Plant Biol* 60:239-260

721 Macintyre HL, Kana TM, Anning T, Geider RJ (2002) Photoacclimation of  
 722 photosynthesis irradiance response curves and photosynthetic pigments in  
 723 microalgae and cyanobacteria. *J Phycol* 38:17-38

724 Méléder V, Rincé Y, Barillé L, Gaudin P, Rosa P (2007). Spatio-temporal changes in  
 725 microphytobenthos assemblages in a macrotidal flat (Bourgneuf Bay, France). *J*  
 726 *Phycol* 43: 1177–1190

727 Migné A, Spilmont N, Davoult D (2004) In situ measurements of benthic primary  
 728 production during emersion: seasonal variations and annual production in the  
 729 Bay of Somme (eastern English Channel, France). *Cont Shelf Res* 24:1437-1449

730 Miles A, Sundbäck K (2000) Diel variation in microphytobenthic productivity in areas  
 731 of different tidal amplitude. *Mar Ecol Prog Ser* 205:11-22



732 Mouget J-L, Perkins R, Consalvey M (2008) Migration or photoacclimation to prevent  
 733 high irradiance and UV-B damage in marine microphytobenthic communities.  
 734 *Aquat Microb Ecol* 52:223-232

735 Müller P, Li XP, Niyogi KK (2001) Non-photochemical quenching. A response to  
 736 excess light energy. *Plant Physiol* 125:1558-1566

737 Nishiyama Y, Allakhverdiev SI, Murata N (2006) A new paradigm for the action of  
 738 reactive oxygen species in the photoinhibition of photosystem II. *Biochim*  
 739 *Biophys Acta* 1757:742-749

740 Olaizola M, Yamamoto HY (1994) Short-term response of the diadinoxanthin cycle and  
 741 fluorescence yield to high irradiance in *Chaetoceros muelleri*  
 742 (Bacillariophyceae). *J Phycol* 30:606-612

743 Owens TG (1986) Light-harvesting function in the diatom *Phaeodactylum tricornutum*  
 744 II. Distribution of excitation energy between the photosystems. *Plant Physiol*  
 745 80:732-738

746 Owens TG, Wold ER (1986) Light-harvesting function in the diatom *Phaeodactylum*  
 747 *tricornutum* I. Isolation and characterization of pigment-protein complexes.  
 748 *Plant Physiol* 80:732-738

749 Oxborough K, Hanlon ARM, Underwood GJC, Baker NR (2000) In vivo estimation of  
 750 the photosystem II photochemical efficiency of individual microphytobenthic  
 751 cells using high-resolution imaging of chlorophyll a fluorescence. *Limnol*  
 752 *Oceanogr* 45:1420-1425

753 Perkins RG, Mouget J-L, Lefebvre S, Lavaud J (2006) Light response curve  
 754 methodology and possible implications in the application of chlorophyll  
 755 fluorescence to benthic diatoms. *Mar Biol* 149:703-712.



- Perkins RG, Lavaud J, Serôdio J, Mouget, J-L, Cartaxana P, Rosa P, Barillé L, Brotas V, Jesus BM (2010) Vertical cell movement is the primary response of intertidal benthic biofilms to increasing light dose. *Mar Ecol Prog Ser* 416:93–103
- Perkins RG, Kromkamp J, Serôdio J, Lavaud J, Jesus B, Mouget J-L, Lefebvre S, Forster R. The application of variable chlorophyll fluorescence to microphytobenthic biofilms. *In* Sugget D, Prasil O, Borowitzka MA (eds) *Chlorophyll a Fluorescence in Aquatic Sciences: Methods and Applications, Series: Developments in Applied Phycology Vol. 4-Chapter 12*, Springer, pp 237-276.
- Rijstenbil, JW (2005) UV- and salinity-induced oxidative effects in the marine diatom *Cylindrotheca closterium* during simulated emersion. *Mar Biol* 147:1063-1073
- Ritchie RJ (2008) Fitting light saturation curves measured using modulated fluorometry. *Photosynth Res* 96:201-15
- Roháček K (2010) Method for resolution and quantification of components of the non-photochemical quenching ( $q_N$ ). *Photosynth Res* 105:101-113
- Roncarati F, Rijstenbil JW, Pistocchi R (2008) Photosynthetic performance, oxidative damage and antioxidants in *Cylindrotheca closterium* in response to high irradiance, UVB radiation and salinity. *Mar Biol* 153:965-973
- Ruban, AV, Lavaud, J, Rousseau, B, Guglielmi, G, Horton, P, Etienne, AL (2004) The super-excess energy dissipation in diatom algae: comparative analysis with higher plants. *Photosyn Res* 82:165-175
- Salleh S, McMinn A (2011) The effects of temperature on the photosynthetic parameters and recovery of two temperate benthic microalgae, *Amphora cf. coffeaeformis* and *cocconeis cf. sublittoralis* (Bacillariophyceae). *J Phycol* 47:1413-1424



780 Serôdio J (2004) Analysis of variable chlorophyll fluorescence in microphytobenthos  
 781 assemblages: implications of the use of depth-integrated measurements. *Aqua*  
 782 *Microb Ecol* 36:137-152

783 Serôdio J, Cruz S, Vieira S, Brotas V (2005) Non-photochemical quenching of  
 784 chlorophyll fluorescence and operation of the xanthophyll cycle in estuarine  
 785 microphytobenthos. *J Exp Mar Biol Ecol* 326:157-169

786 Serôdio J, Lavaud J (2011) A model for describing the light response of the non-  
 787 photochemical quenching of chlorophyll fluorescence. *Photosynth Res* 108:61-  
 788 76

789 Serôdio J, Vieira S, Cruz S, Coelho H (2006) Rapid light-response curves of  
 790 chlorophyll fluorescence in microalgae: relationship to steady-state light curves  
 791 and non-photochemical quenching in benthic diatom-dominated assemblages.  
 792 *Photosynth Res* 90:29-43

793 Serôdio J, Catarino, F (1999) Fortnightly light and temperature variability on estuarine  
 794 intertidal sediments and implications for microphytobenthos primary  
 795 productivity. *Aquat Ecol* 33:235-241

796 Serôdio J, Vieira S, Cruz S (2008) Photosynthetic activity, photoprotection and  
 797 photoinhibition in intertidal microphytobenthos as studied in situ using variable  
 798 chlorophyll fluorescence. *Cont Shelf Res* 28:1363-1375

799 Underwood GJC (2002) Adaptations of tropical marine microphytobenthic assemblages  
 800 along a gradient of light and nutrient availability in Suva Lagoon, Fiji. *Eur J*  
 801 *Phycol* 37:449-462

802 Underwood GJC, Kromkamp J (1999) Primary production by phytoplankton and  
 803 microphytobenthos in estuaries. *Adv Ecol Res* 29:93-153



Underwood GJC, Perkins RG, Consalvey MC, Hanlon ARM, Oxborough K, Baker NR,  
 Paterson, DM (2005) Patterns in microphytobenthic primary productivity:  
 Species-specific variation in migratory rhythms and photosynthetic efficiency in  
 mixed-species biofilms. *Limnol Oceanogr* 50:755-767

Van Leeuwe MA, Brotas V, Consalvey M, Forster RM, Gillespie D, Jesus B,  
 Roggeveld J, Gieskes WWC (2008) Photoacclimation in microphytobenthos and  
 the role of xanthophyll pigments. *Eur J Phycol* 43:123-132

Walters RG, Horton P (1991) Resolution of components of non-photochemical  
 chlorophyll fluorescence quenching in barley leaves. *Photosynth Res* 27:121-133

Waring J, Baker NR, Underwood GJC (2007) Responses of estuarine intertidal  
 microphytobenthic algal assemblages to enhanced ultraviolet B radiation. *Global  
 Change Biol* 13:1398-1413

Waring J, Klenell M, Bechtold U, Underwood GJC, Baker NR (2010) Light-induced  
 responses of oxygen photoreduction, reactive oxygen species production and  
 scavenging in two diatom species. *J Phycol* 46:1206-1217

Wu H, Cockshutt AM, McCarthy A, Campbell DA (2011) Distinctive photosystem II  
 photoinactivation and protein dynamics in marine diatoms. *Plant Physiol*  
 156:2184-2195



823	Table 1. Notation
824	
825	$\alpha$ , initial slope of the ETR vs $E$ curve
826	$a, b, c$ , parameters of the Eilers and Peeters (1988) model
827	DTT, dithiothreitol
828	$\Delta F/F_m'$ , effective quantum yield of PSII
829	DD, diadinoxanthin
830	DT, diatoxanthin
831	DDE, diadinoxanthin de-epoxidase
832	$E$ , PAR irradiance
833	$E_{50}$ , Irradiance level corresponding to 50% of $NPQ_m$ in a NPQ vs $E$ curve
834	$E_k$ , photoacclimation parameter of an ETR vs $E$ curve
835	ETR, PSII electron transport rate
836	$ETR_m$ , maximum ETR level in an ETR vs $E$ curve
837	$F_o, F_m$ , Minimum and maximum fluorescence of a dark-adapted sample
838	$F_s, F_m'$ , Steady state and maximum fluorescence of a light-adapted sample
839	Lat A, Latrunculin A
840	$n$ , sigmoidicity coefficient of the NPQ vs $E$ curve
841	NPQ, non-photochemical quenching



842	$\text{NPQ}_m$ , maximum NPQ level in a NPQ vs $E$ curve
843	PAR, photosynthetically active radiation
844	PSII, photosystem II
845	$q_E$ , energy-dependent quenching
846	$q_I$ , photoinhibitory quenching
847	$t$ , time during recovery following light stress
848	XC, xanthophyll cycle
849	



Table 2. Extent of photoinhibition and efficiency of photoprotection (%), calculated as percentage of  $\Delta F/F_m'$  recovery after 10.5 min. Relative contributions of vertical migration and of the xanthophyll cycle to overall photoprotection (%), as calculated from the reduction of the  $\Delta F/F_m'$  recovery in samples treated with Lat A and with Lat A and DTT, respectively, relatively to control samples. Mean and standard error of three replicates. Numbers within parenthesis indicate results obtained when considering 6 and 15 min of recovery, respectively.

	May	October
Photoinhibition	$12.3 \pm 0.55$ (16.6, 11.7)	$22.0 \pm 2.79$ (33.7, 17.0)
Recovery	$87.7 \pm 0.55$ (83.4, 88.3)	$78.0 \pm 2.79$ (66.3, 83.0)
Vertical migration	10.6 (24.0, 3.6)	14.3 (17.0, 11.7)
Xanthophyll cycle	10.1 (6.4, 13.2)	7.2 (7.3, 5.8)
Others	79.3 (69.5, 83.2)	78.5 (75.7, 82.5)



## Figure legends

Fig. 1. Light-response curves of ETR (A) and NPQ (B) measured in May and October 2010. Mean of six replicates. Vertical bars: one standard error. Numbers represent the mean values of model parameters estimated for light-response curves measured for each individual sample.

Fig. 2. Variation of migration inhibition with the concentration of added Lat A solution. Mean of three replicates. Vertical bars: one standard error. Line represents the fit of exponential decay model.

Fig. 3. Inhibition of NPQ as a function of concentration of added DTT solution. NPQ induced upon exposure to  $400 \mu\text{mol quanta m}^{-2} \text{s}^{-1}$ . Mean of three replicates. Vertical bars: one standard error. Line represents the fit of exponential decay model.

Fig. 4. Light stress-recovery experiment. Variation of PSII quantum yield,  $\Delta F/F_m'$ , during sequential exposure to low light (pre-stress,  $55 \mu\text{mol quanta m}^{-2} \text{s}^{-1}$ ), light stress under high light (high light,  $1200 \mu\text{mol quanta m}^{-2} \text{s}^{-1}$ , 180 min) and recovery under low light (recovery,  $55 \mu\text{mol quanta m}^{-2} \text{s}^{-1}$ , 10.5 min) for controls and for samples treated with migration inhibitor Lat A and with migration and xanthophyll cycle inhibitors (Lat A + DTT), collected in May 2010. Mean of three replicates. Vertical bars: one standard error.

Fig. 5. Images of PSII quantum yield,  $\Delta F/F_m'$  (false color scale), as measured in the sediment samples used in the light stress experiment described in Fig. 4 at the end of



first low light exposure (pre-stress,  $55 \mu\text{mol quanta m}^{-2} \text{s}^{-1}$ ), at the end of high light exposure (high light,  $1200 \mu\text{mol quanta m}^{-2} \text{s}^{-1}$ , 180 min) and following recovery under low light (recovery,  $55 \mu\text{mol quanta m}^{-2} \text{s}^{-1}$ , 10.5 min). Three replicated areas of interest for each treatment.

Fig. 6. Images of fluorescence level  $F_s$  (false color scale) as measured in the sediment samples used in the light stress experiment described in Fig. 4. at the end of first low light exposure (pre-stress,  $55 \mu\text{mol quanta m}^{-2} \text{s}^{-1}$ ), and after recovery following end of high light exposure (high light,  $1200 \mu\text{mol quanta m}^{-2} \text{s}^{-1}$ , 180 min; recovery,  $55 \mu\text{mol quanta m}^{-2} \text{s}^{-1}$ , 10.5 min). Three replicated areas of interest for each treatment.

Fig. 7. Recovery of PSII quantum yield,  $\Delta F/F_m'$ , during relaxation following light stress for control samples and for samples treated with migration inhibitor Lat A and with migration and xanthophyll cycle inhibitors (Lat A + DTT). Lines represent the exponential model described by Eq. (6) fitted to average  $\Delta F/F_m'$  values. Detail of Fig. 4.

Fig. 8. Efficiency of photoprotection, as percentage of recovery after 10.5 min low light following high light exposure, in May and October, for controls and inhibitor-treated samples. Mean of three replicates. Vertical bars: one standard error.



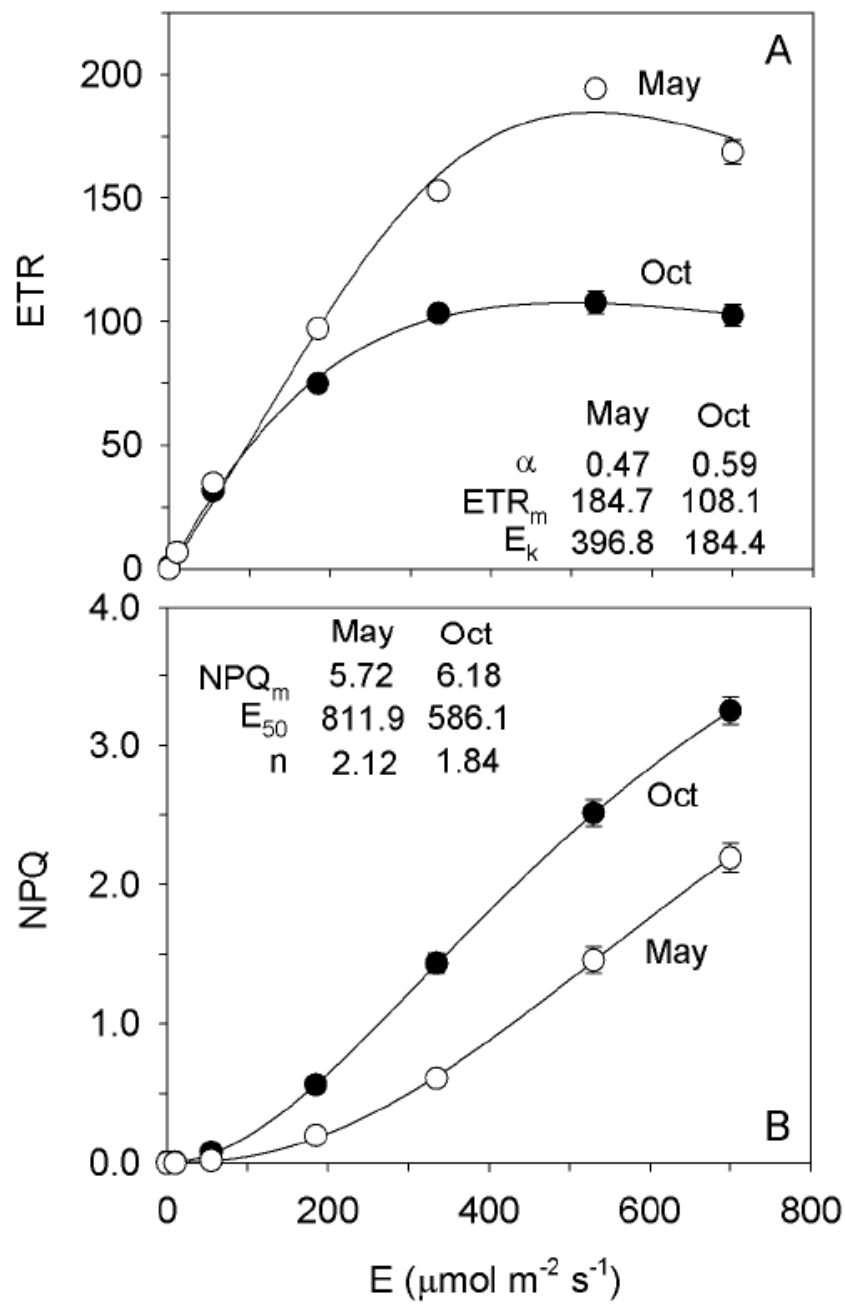




Figure 2

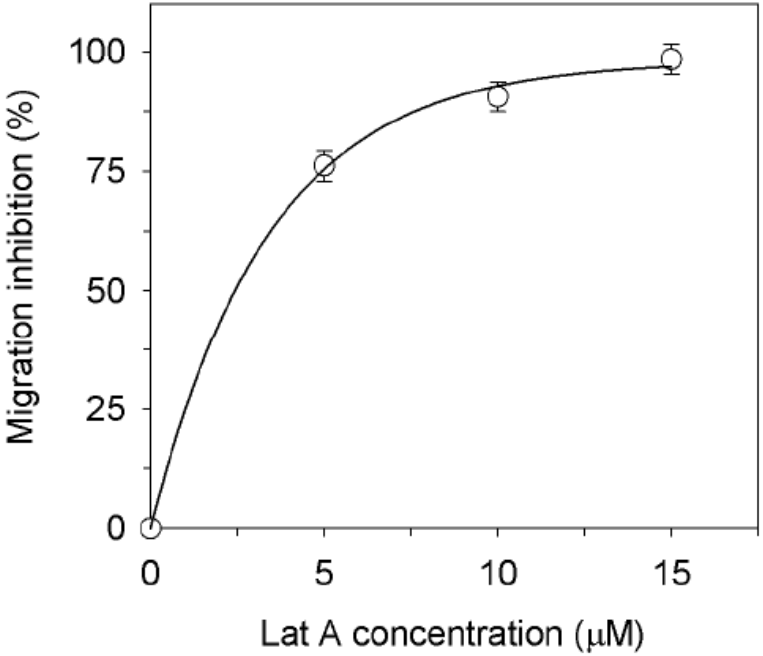




Figure 3

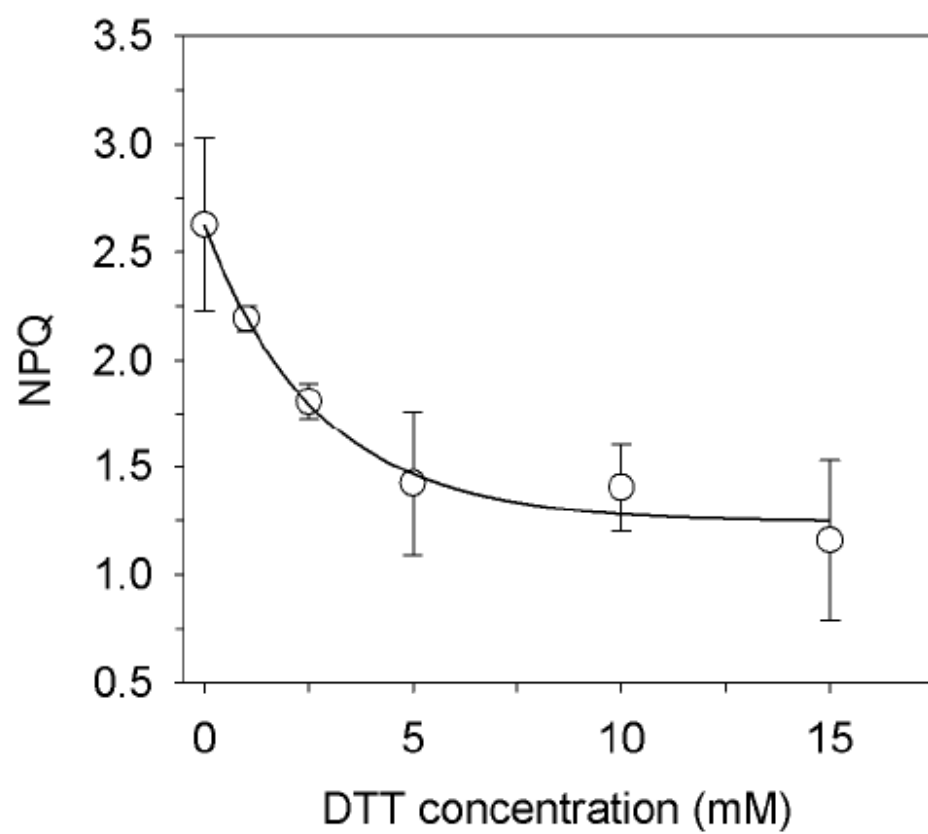




Figure 4

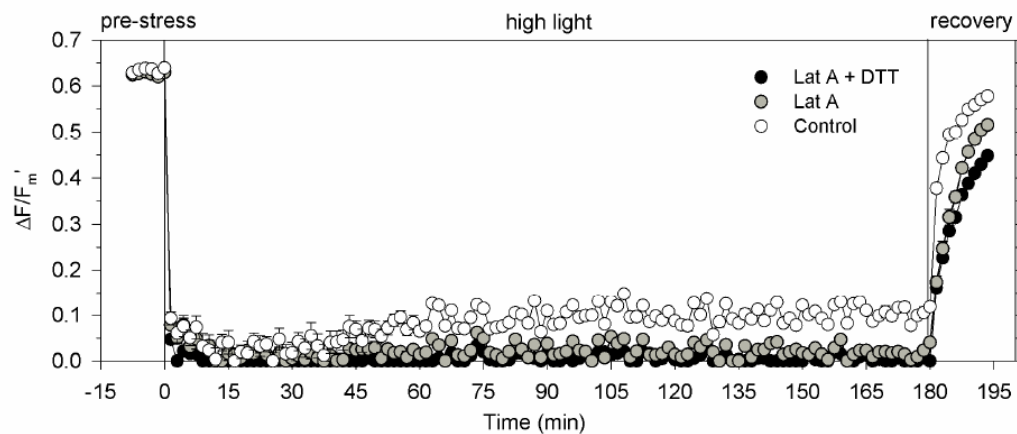
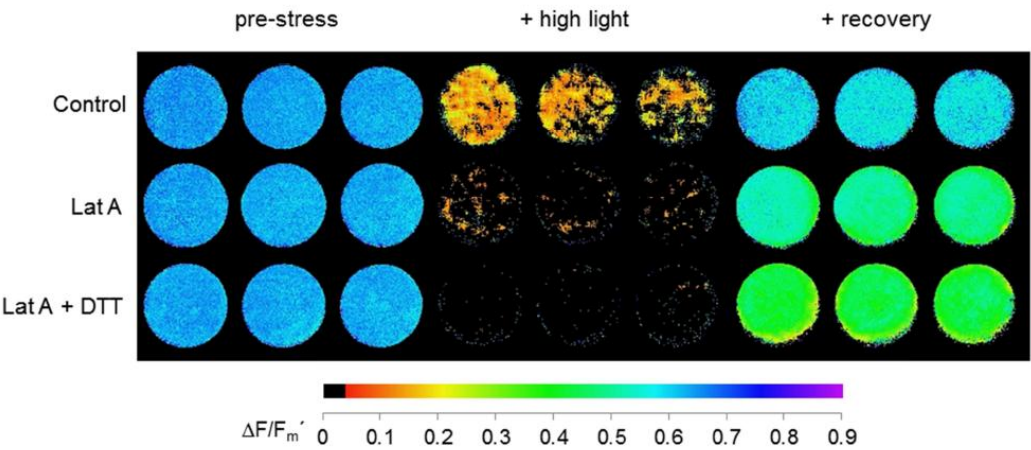




Figure 5





923

924

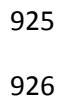
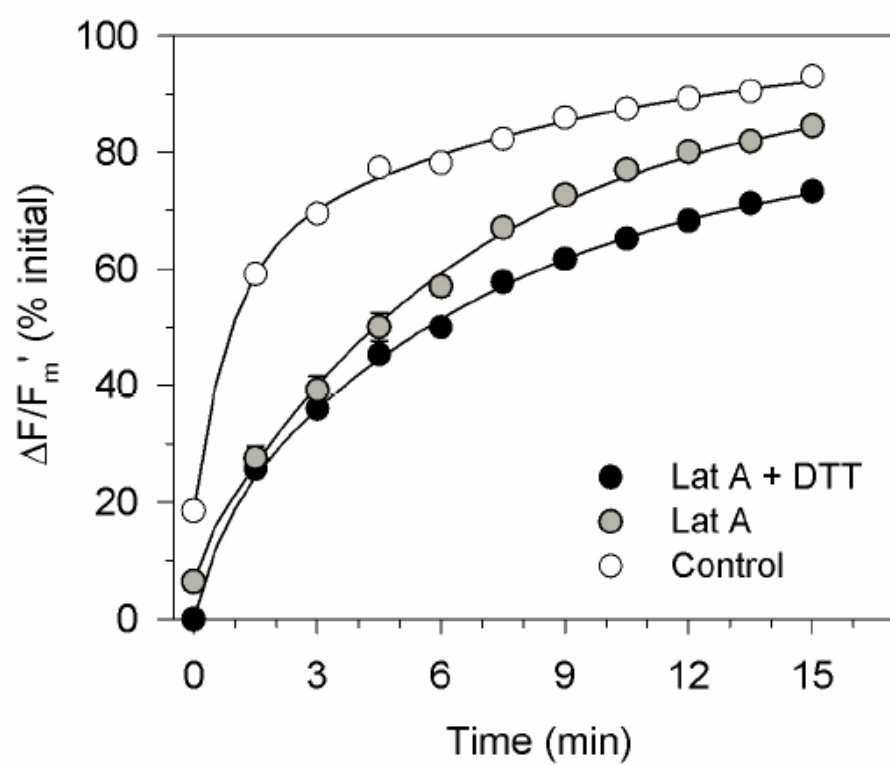




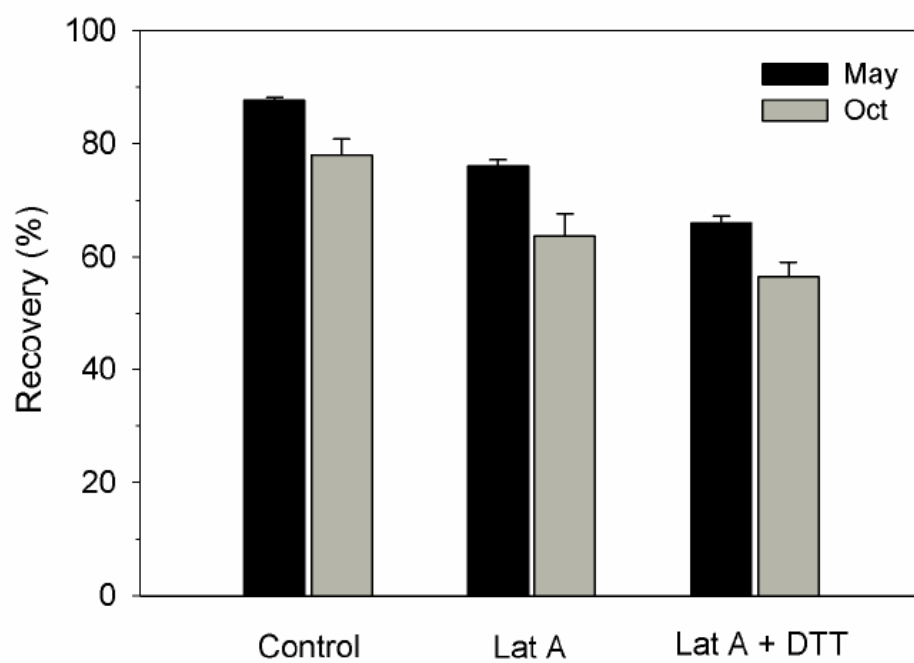
Figure 7





931 Figure 8

932



933